Trends in element incorporation in hyaline and porcelaneous foraminifera as a function of pCO_2

Inge van Dijk[1], Lennart J. de Nooijer[1], Gert-Jan Reichart[1,2]

[1]Department of Ocean Systems, NIOZ-Royal Netherlands Institute for Sea Research, Postbus 59, 1790 AB, Den Burg, the Netherlands, and Utrecht University.

[2]Faculty of Geosciences, Earth Sciences Department, Utrecht University, Budapestlaan 4, 3584 CD, Utrecht, the Netherlands

Abstract

In this study we analyzed the impact of seawater carbonate chemistry on the incorporation of elements in both hyaline and porcelaneous larger benthic foraminifera. We observed a higher incorporation of Zn and Ba when pCO_2 increases from 350 to 1200 ppm. Modelling the activity of free ions as a function of pCO_2, shows that speciation of some elements (like Zn and Ba) are mainly influenced by the formation of carbonate complexes in seawater. Hence, differences in foraminiferal uptake of these might be related primarily by the speciation of these elements in seawater. We investigated differences in trends in element incorporation between hyaline (perforate) and porcelaneous (imperforate) foraminifera in order to unravel processes involved in element uptake and subsequent foraminiferal calcification. In hyaline foraminifera we observed a correlation of element incorporation of different elements between species, reflected by a general higher built-in of elements in species with higher Mg content. Between porcelaneous species inter-element differences are much smaller. Besides these contrasting trends in element incorporation, however, similar trends are observed in element incorporation as a function of seawater carbonate chemistry in both hyaline and porcelaneous species. This hints at similar mechanisms responsible for the transportation of ions to the site of calcification for these groups of foraminifera, although the contribution of these processes might differ across species.

1. Introduction

Calcareous foraminifera, cosmopolitan unicellular protists, are widely used to reconstruct past environmental conditions, since the chemical composition of the carbonate shells reflect a wide variety of environmental parameters. For instance, the Mg/Ca of foraminiferal shells is primarily determined by seawater temperature (Nürnberg et al., 1996; Allen and Sanders, 1994) and seawater Mg/Ca (Segev and Erez, 2006; Evans et al., 2015) and has been widely applied as a paleothermometer (Elderfield and Ganssen, 2000; Lear et al., 2000). The use of foraminifera as proxies for the inorganic carbon system in the past (seawater pH, alkalinity, saturation state, etc.) has more recently been added to the foraminiferal proxy tool-box. For example, the concentrations of trace elements in foraminiferal shells, including U (Keul et al., 2013; Russell et al., 2004), Zn (Marchitto et al., 2000; van Dijk et al., 2017) and B (Yu and Elderfield, 2007) correlates to seawater carbonate ion concentration ($[CO_3^{2-}]$), while the boron isotopic composition of foraminiferal calcite used as a proxy for pH (Sanyal et al., 1996). However, insight in vital effects (Erez, 2003) and inter-specific differences in trace element incorporation (Bentov and Erez, 2006; Toyofuku et al., 2011; Wit et al., 2012) is needed to increase robustness of these proxies.

On the broadest taxonomic scale foraminifera produce tests using either one of two fundamentally different mechanisms. These calcification strategies reflect the evolutionary separation of foraminiferal groups dating back to the Cambrian diversification, from where the imperforate porcelaneous species and perforate hyaline foraminifera, developed independently (Pawlowski et al., 2003). Previously observed species-specific differences in partitioning and fractionation of elements most likely primarily reflect these differences in calcification strategy, since these offsets are largest between hyaline and porcelaneous species (see for a summary, Toyofuku et al., 2011). The calcification process of the latter group has been studied more extensively than that of the porcelaneous species (De Nooijer et al., 2014). Although many aspects of perforate calcification remain unsolved, there is consensus that chamber formation takes place extracellularly, but within a (semi-) enclosed space, generally termed the site of calcification (SOC). The first layers of calcite precipitate on an organic matrix (the POS or primary organic sheet) that serves as a template for the calcite layer that forms the chamber wall (Erez, 2003; Hemleben et al., 1977). To promote calcification, foraminifera furthermore need to remove Mg ions

and/or protons (Zeebe and Sanyal, 2002) from the seawater entering the SOC. A number of larger benthic foraminifera form hyaline shells, although the amount of Mg in their shells is often more than 10 times higher than that of planktonic and small benthic hyaline species, hence covering a larger range in $Mg/Ca_{CALCITE}$ values. The calcification strategy of porcelaneous foraminifera is less well studied, which may be partly explained by their limited application in paleoceanography. Porcelaneous foraminifera use a different mode of calcification (Debenay et al., 1998; De Nooijer et al., 2009; Berthold, 1976; Hemleben et al., 1986) and produce shells without pores (hence, the term imperforate) consisting of tablets or needles (Erez, 2003; Bentov and Erez, 2006; Debenay et al., 1998). These calcitic needles (2-3µm) are precipitated intracellularly (Berthold, 1976), after which they are transported out of the foraminifer to form a new chamber (Angell, 1980). At the outer and inner layers of these chambers, the needles are arranged along the same orientation so that they form an optically homogenous surface, giving it a shiny (hence the term 'porcelaneous') appearance. In general the Mg/Ca values of the shells of porcelaneous foraminifera are high.

Remarkably, despite this large biological control, incorporation of minor and trace elements still reflects environmental conditions, in both hyaline and porcelaneous foraminiferal shells. Systematic offsets between different species, interdependence of trace elements incorporated (Langer et al., 2016) and the different response of element incorporation on element speciation (Wit et al., 2013; Keul et al., 2013; van Dijk et al., 2017), potentially provides useful clues for determining which processes play an important role in the biomineralization pathways. Here we present the results from a controlled growth experiment for which we used several (intermediate- and high-Mg) hyaline and porcelaneous species combined with an inter-species comparison of trace element incorporation. We assessed the impact of bio-calcification on element incorporation as a function of pCO_2 in order to explore the proposed inorganic carbonate proxies (e.g. Zn/Ca; van Dijk et al., 2017) and the impact of different calcification strategies (hyaline versus porcelaneous) on element partitioning. We cultured eight benthic foraminiferal species (4 hyaline and 4 porcelaneous) under four different pCO_2 conditions, analyzing incorporation of Mg, Sr, Na, Zn and Ba.

2. Methods

2.1. Foraminiferal collection

Large samples of macroalgae (*Dictyota* sp.) were collected in November 2015 at a depth of 2-3 meters in Gallows Bay, St. Eustatius (N 17°28'31.6", W62°59'9.4"). Salinity was ~34 and temperature was ~29°C at the site of collection. The collected macroalgae were transported to the laboratory at the Caribbean Netherlands Science Institute (CNSI), where they were placed in a 5 L aquarium with aerated and unfiltered seawater. From this stock, small amounts of algae and debris were gently sieved over a 90 and 600 µm mesh to carefully dislodge foraminifera. Several species of foraminifera were picked from the resulting 90-600 µm fraction and directly from the macroalgae. Living specimens of *Sorites marginalis* (Lamarck, 1816), *Amphistegina gibbosa* (d'Orbigny, 1839), *Laevipeneroplis bradyi* (Cushman, 1930) and *Archaias angulatus* and limited amounts (<20) of *Peneroplis pertusus* (Forskål, 1775), *Asterigerina carinata* (d'Orbigny, 1839), *Heterostegina antillarum* (d' Orbigny, 1839), and *Planorbulina acervalis* (Brady, 1884) characterized by yellow cytoplasm and pseudopodial activity, were selected for the culturing experiments.

2.2. Culture set-up

Four barrels, each filled with 100 L of seawater (5µm filtered), were connected to a Li-Cor CO_2/H_2O analyzer (LI-7000), to regulate the CO_2 level in the barrels' head space. The set-points were maintained by addition of CO_2 and/ or CO_2-scrubbed air according to the monitored pCO_2. The set-points for pCO_2 were 350, 450, 760 and 1400 ppm resulting in four batches of seawater (treatment A-D) differing only in their inorganic carbon chemistry. Salinity (34.0±0.2) was monitored with a salinometer (VWR CO310). The fluorescent compound calcein (Bis[N,N-bis(carboxymethyl)aminomethyl]-fluorescein) was added to the culture media (5 mg/L seawater) to enable determination of newly formed chambers during the culture experiment (Bernhard et al., 2004). Short-term exposure (<three weeks) to calcein has no detectable impact on the physiology of benthic foraminifera (Kurtarkar et al., 2015), and the presence of calcein has no effect on the incorporation of Mg and Sr in foraminiferal calcite (Dissard et

al., 2009). Culture media was stored air-free in portions of 250 ml in Nalgene bottles with teflon lined caps at 4°C until further use.

Foraminifera were divided over the different treatments in duplicate and placed in 70 ml Falcon® tissue bottles with gas-tight caps in a thermostat set at 25°C (Fig. 1). The thermostat was monitored by a temperature logger (Traceable Logger Trac, Maxi Thermal), recording the temperature every minute. The average temperature over the whole experiment was 25 ±0.2°C. To create uniform light conditions, the thermostat was equipped with two LED shelfs, which resulted in high light conditions 12 hr/12hr. Culture media was replaced every four days, to avoid build-up of organic waste and to obtain stable seawater element concentrations and carbon chemistry. Foraminifera were fed after every water change with 0.5 ml of concentrated freeze-dried *Dunaliella salina* cells, pre-diluted with the corresponding treatment seawater. After 21 days, the experiment was terminated. Foraminifera were rinsed three times with de-ionized water, dried at 40°C and stored in micropaleontology slides until further analysis at the Royal Netherlands Institute for Sea Research (NIOZ).

2.3. Analytical methods

2.3.1. Seawater carbon parameters

At the start and termination of the experiment, 125 ml samples of the seawater at each of the different experimental conditions were collected to analyze dissolved inorganic carbon (DIC) and total alkalinity (TA) on a Versatile INstrument for the Determination of Titration Alkalinity (VINDTA) at the CNSI. Using the measured DIC and TA values and the software CO2SYS v2.1, adapted to Excel by Pierrot et al. (2006) the other carbon parameters (including $[CO_3^{2-}]$ and $\Omega_{CALCITE}$) were calculated. For this we used the equilibrium constants for K1 and K2 from Lueker et al. (2000) and $KHSO_4$ from (Dickson, 1990) (Table 1).

2.3.2. Seawater element concentrations

At the start and end of the experiment and during replacement of the culture media, subsamples were collected in duplo using 50 ml LDPE Nalgene bottles and immediately frozen at -80^{0}C. After transportation to the NIOZ, defrosted samples were acidified with 3 times Quartz distilled HCl to pH ~1.8 and the seawater composition of the samples was analyzed on an Element 2 sector field double focusing mass spectrometer (SF-ICP-MS) run in medium resolution mode. IAPSO (International Association for the Physical Sciences of the Ocean) Standard Seawater was used as a drift monitor. Analytical precision (relative standard deviation) was 3% for Ca, 4% for Mg, 1% Na, 1% for Sr and 5% Ba. We obtained average values of 5.25±0.06 mol/mol for Mg/Ca, 44.6±0.6 mol/mol for Na/Ca, 8.63±0.05 mol/mol for Sr/Ca, and 9.04±0.47 µmol/mol for Ba/Ca.

A subsample was analyzed using a commercially available pre-concentration system, SeaFAST S2. With the SeaFAST system elements with low concentrations are pre-concentrated to values above detection limit of the SF-ICP-MS. Accordingly, we measured Cd, Pb U, B, Ti, Mn, Fe, Co, Ni, Cu, and Zn. In short, 10ml of sample was mixed with an ammonium acetate buffer to pH 6.2 and loaded on a column containing NOBIAS chelating agent. After rinsing the column with a diluted ammonium acetate buffer the metals were eluted in 750 µl of quartz distilled 1.5 M HNO_3 before being quantified on the SF-ICP-MS. Here we use the Zn data only, as this was analyzed in the foraminifera as well. Analytical precision (relative standard deviation) was 5% for Zn. We obtained an average value of 15.3±0.5 µmol/mol for seawater Zn/Ca for all treatments. Although these values are clearly above natural open ocean values, the concentrations are very uniform between treatments and when comparing start and end of the experiments. The contamination with Zn might hence have occurred already when filling the culture setup with the waters from the bay adjacent to the culture facility. Concentrations are well below values considered harmfull for formainifera (Nardelli et al., 2016).

2.3.3. Cleaning methods

After termination of the experiment, foraminiferal shells were cleaned following an adapted version of Barker et al. (2003). Per treatment duplicate, all foraminifera were transferred to 10 ml polyethylene

vials. To each vial, 10 mL 1% H_2O_2 solution (buffered with 0.5M NH_4OH) was added to remove organic matter. The vials were heated for 10 minutes in a water bath at 95 °C, and placed in an ultrasonic bath for 30 seconds (degas mode, 80kHz, 50% power), after which the oxidizing reagent was removed. These steps (organic removal procedure) were repeated five times. Foraminiferal samples were rinsed five times with ultrapure water, after which the vials were stored overnight in a laminar flow cabinet at room temperature to dry. Dried foraminifera were placed on double sided tape on LA-ICP-MS stubs. Pictures were taken of individual foraminifera with a ZEISS Axioplan 2 fluoresence microscope equipped with appropriate excitation and emission optics and a ZEISS Axiocam MRc 5 camera, to assess the number of chambers added during the experiment based on the incorporation of calcein.

2.3.4. LA-ICP-MS

Element concentrations of individual fluorescent chambers were analyzed by Laser Ablation-ICP-MS (Reichart et al., 2003; van Dijk et al., 2017). To determine foraminiferal element concentrations, the laser system (NWR193UC, New Wave Research) at the Royal NIOZ was equipped with a Two Volume 2 cell (New Wave Research), characterized by a wash-out time of 1.8 seconds (1% level) and hence allowing detection of variability of obtained element to Ca ratios within chamber walls. Single chambers were ablated in a helium environment using a circular laser spot with a diameter of 80 µm (*S. marginalis*) or 60 µm (other species). We ablated all calcein-stained chambers twice, except for the first 1-2 chambers that formed during the experiment to avoid contamination of calcite of chambers formed prior to the experiments and overlapped by the labelled chambers (Fig.2).

All foraminiferal samples were ablated with an energy density of 1±0.1 J/cm^2 and a repetition rate of 6 Hz. The resulting aerosol was transported on a helium flow through an in house build smoothing device, being mixed with a nitrogen flow (5 ml/min), before entering the quadrupole ICP-MS (iCAP-Q, Thermo Scientific). Monitored masses included ^{7}Li, ^{11}B, ^{23}Na, ^{24}Mg, ^{25}Mg, ^{27}Al, ^{43}Ca, ^{44}Ca, ^{66}Zn, ^{88}Sr and ^{137}Ba. Contrary to ^{67}Zn and ^{68}Zn, ^{66}Zn is free of interferences when measuring calcium carbonate and SRM NIST (National Institute of Standard and Technology, U.S., Standard Reference Material) glass

standards (Jochum et al., 2012). Potential contamination or diagenesis of the outer or inner layer of calcite was excluded by monitoring the Al signal. At the start of each series, we analyzed SRM NIST612 and NIST610 glass standard in triplicate (using an energy density of 5±0.1 J/cm^2), JCt-1 (coral carbonate) and two in-house standards, namely NFHS (NIOZ Foraminifera House Standard; Mezger et al., 2016) and the Iceland spar NCHS (NIOZ Calcite House Standard). We further analyzed JCp-1 (coral, Porites sp.; Okai et al., 2002) and MACS-3 (Synthetic Calcium Carbonate) at the start of each series, and to monitor drift after every ten samples. All element to calcium ratios were calculated with an adapted version of the MATLAB based program SILLS (Signal Integration for Laboratory Laser Systems; Guillong et al., 2008). SILLS was modified by NIOZ to evaluate LA-ICP-MS measurements on foraminifera, allowing import of Thermo Qtegra software sample list, laser data reduction and laser LOG files. Major adaptions include improved automated integration and evaluation of (calibration and monitor) standards, quality control report of the monitor standards and export in element to calcium ratios (mmol/mol). Calibration was performed against the MACS-3 carbonate standard, with ^{43}Ca as an internal standard and we used the multiple measurements of MACS-3 for a linear drift correction. Relative analytical precision (relative standard deviation (RSD) of all MACS-3 analyses) is 3% for ^{23}Na, 3% for ^{24}Mg, 3% for ^{25}Mg, 4% for ^{66}Zn, 3% for ^{88}Sr and 3% for ^{137}Ba. In total, 961 analyses were performed on 251 specimens covering eight species cultured in four experimental conditions (see Table 2 for details).

We calculated the standard deviation (SD), RSD and standard error (SD/√n; SE) per treatment. The partitioning coefficient (D) of an element (E) between seawater and foraminiferal calcite is expressed as $D_E = (E/Ca_{CALCITE})/(E/Ca_{SW})$. Partition coefficients and element versus calcium ratio parameters were statistically compared with different experimental parameters (such as pCO_2 or $[CO_3^{2-}]$) using a two-sided t-test with 95% confidence levels. This also allows for the calculation of 95% confidence intervals over the average per treatment. Pairwise comparisons were made for per E/Ca per species and culture conditions using ANOVA. Groups that showed significant difference were assigned different letters. When comparing partition coefficients to other studies, E/Ca_{SW} data was, in some studies, not measured.

For these studies we used average seawater E/Ca_{SW} to calculate D_E (see also supplementary Table 1), allowing comnparing partitioning coefficients.

3. Results

3.1. Element/Ca as a function of ocean acidification

In hyaline species $Mg/Ca_{CALCITE}$ varies between 25.9-141.3 mmol/mol Mg/Ca. In contrast, $Mg/Ca_{CALCITE}$ of porcelaneous species ranges from 121.3-149.3 mmol/mol (Table 3). This large spread in foraminifera E/Ca of hyaline species is also observed for Sr (1.7-3.1 mmol/mol), Na (3.4-19.5 mmol/mol), Zn (9.0-97.0 µmol/mol) and Ba (2.7-20.1 µmol/mol), while porcelaneous species only vary over a narrow range (Sr = 2.0-2.2 mmol/mol; Na = 3.8-5.8 mmol/mol; Zn = 53.0-140.8 µmol/mol; Ba = 18.0-29.0 µmol/mol).

In both porcelaneous and hyaline species we find an increase of $Zn/Ca_{CALCITE}$ and $Ba/Ca_{CALCITE}$ with pCO_2, while foraminiferal Sr/Ca, Mg/Ca and Na/Ca remain similar across the experimental conditions (Fig. 3 and Table 4). Sensitivity of both foraminiferal Zn/Ca and Ba/Ca to changes in seawater pCO_2 differs between the studied porcelaneous and hyaline species. When pCO_2 changes from 350 to 1200 ppm, Zn/Ca of hyaline foraminifera increase by a factor of 3.7 (*A. carinata*) or 4.5 (*A. gibbosa*) while porcelaneous foraminiferal Zn/Ca increases only by 1.3 (*S. marginalis*), 1.8 (*A. angulatus*) and 2.1 (*L. bradyi*). Also sensitivity of foraminiferal Ba/Ca to the same change in pCO_2 shows a similar pattern, with Ba/Ca of hyaline species increasing by a factor of 3.6 (*A. carinata*) or 3.7 (*A. gibbosa*), while porcelaneous species increase Ba/Ca only with a factor of 1.8 (*S. marginalis*), 1.6 (*A. angulatus*) or 2.1 (*L. bradyi*).

3.2. Inter-species differences in element incorporation

When comparing Mg incorporation to that of the other elements studied here (Ba, Zn, Sr and Na) between hyaline species (treatment B; Table 3), we observe a positive relation between D_{Mg} with D_{Sr} ($p<0.0025$), D_{Na} ($p<0.0005$), D_{Ba} ($p<0.05$) and D_{Zn} ($p<0.005$). In general hyaline species are enriched

similarly in all elements (Fig. 4). Compared to porcelaneous species, the hyaline shell building species which incorporate most Mg (>100 mmol/mol Mg/Ca) incorporate more Na, and Sr, while incorporating less Zn and Ba. Element incorporation across porcelaneous species is less variable than observed for hyaline species. Including data from literature (both culture and field calibrations; see supplementary Table S1), preferable in which both Mg/Ca and at least one other element (Na, Sr, Ba or Zn) is measured, shows that the relation based on the Caribbean species studied here is also more general applicable when including more species (D_{Sr} = $p<0.005$; D_{Na} = $p<0.0005$); D_{Ba} = $p<0.005$; D_{Zn} = $p<0.01$), even though this compiled data (labeled 'All studies' in Tabel S2) covers a somewhat wider range in environmental and experiment conditions.

4. Discussion

4.1. Effect of ocean acidification on Element/Ca

For neither porcelaneous nor hyaline species, foraminiferal Mg/Ca, Na/Ca and Sr/Ca systematically change with pCO_2. The impact of pH (and/or $[CO_3^{2-}]$) on $Mg/Ca_{CALCITE}$ and $Sr/Ca_{CALCITE}$ in foraminifera has been the subject of discussion (e.g., Dissard et al., 2010; Elderfield et al., 1996). In deep-sea benthic species, incorporation of certain elements is governed by carbonate system as observed for Zn by Marchitto et al. (2005) and Cd and Ba by McCorkle et al. (1995). Observed response to changes in carbonation ion concentration are in these studies mainly due to calcification in undersaturated seawater, as described by 'the carbonate ion saturation hypothesis' (Elderfield et al., 2006). In some low-Mg benthic species, both $Mg/Ca_{CALCITE}$ and $Sr/Ca_{CALCITE}$ do not seem to depend on inorganic carbon system parameters, e.g. pH or $[CO_3^{2-}]$ (Allison et al., 2011; Dueñas-Bohórquez et al., 2011). However, for several planktonic species pH does influence $Mg/Ca_{CALCITE}$ and $Sr/Ca_{CALCITE}$ (Russell et al., 2004; Lea et al., 1999; Evans et al., 2016). The effect of pH on $Sr/Ca_{CALCITE}$ might be explained via increased growth rates due to pH-associated changes in $[CO_3^{2-}]$ (Dissard et al., 2010). However, due to the limited experimental set-up, we are not able to disentangle the effects of the different carbon parameters in this study. Still, here we show that incorporation of Mg, Sr and Na of the selected larger benthic hyaline and

porcelaneous foraminifera are not significantly impacted when cultured over a limited range of pCO_2 and thus [CO_3^{2-}] and pH values.

In contrast, foraminiferal Zn/Ca and Ba/Ca are significantly impacted by pCO_2 for all species studied here (Table 4; Fig. 3). Although Hönisch et al. (2011) suggested that the impact of carbonate chemistry on Ba incorporation is negligible, their data does suggest a trend over the same interval in pH as studied here. In hyaline foraminifera, Zn/Ca and Ba/Ca increases more as a function of pCO_2 (factor of 3.7-4.5 and 3.6-3.7, respectively when pCO_2 increases from 350 to 1200 ppm) compared to the porcelaneous species (1.3-2.1 and 1.6-2.1 times, respectively). This observation suggests that the mechanisms involved in uptake of Ba and Zn are similar for porcelaneous and hyaline species, although the contribution of this process is different, which leads to differences in the sensitivity of Zn and Ba incorporation with pCO_2

4.2. Speciation in the microenvironment

In the culture set-up used, increasing pCO_2 increases DIC, reduces pH and thereby decreases seawater [CO_3^{2-}]. Speciation of Zn, Ba and also other elements, like U (Keul et al., 2013; Russell et al., 2004; van Dijk et al., 2017), is primarily controlled by seawater [CO_3^{2-}]. The speciation of all elements studied here (Mg, Na, Sr, Zn and Ba) for our different seawater treatments were modelled using PHREEQC, a computer program for speciation, batch-reaction, one-dimensional transport, and inverse geochemical calculations (Parkhurst and Appelo, 1999). For this we used the standard in-software llnl database, a PHREEQC database that implements most of the inorganic aqueous species and minerals in the thermodynamic data and includes many elements not available in any other PHREEQC database. We observed a decrease of free ions (Zn^{2+} and Ba^{2+}) and an increase in Ba and Zn carbonate complexes ($BaCO_3^0$ and $ZnCO_3^0$), with increasing pCO_2 (Fig. 5), while the activity of Mg^{2+}, Na^+ and Sr^{2+} remained similar. This suggests that element incorporation in foraminiferal calcite might be depending on the availability of free ions, which in the case of Ba and Zn, changes with pCO_2. This is contrary to inorganic

precipitation, were carbonate complexes (e.g. $MgCO_3^0$) are easily incorporated into the calcite crystal lattice.

4.3. Trends in element incorporation

Element incorporation in hyaline foraminifera is highly interdependent, i.e. species with increased Mg content also incorporate more Sr, Na, Ba and Zn (Fig. 3). The linear increase in Sr incorporation with increasing Mg/Ca has also been observed for other hyaline species, like *Operculina ammonoides* (Evans et al., 2015), *Amphistegina lessonii* and *Ammonia aomoriensis* (Mewes et al., 2015), which both fall on the same trend as that for inorganic calcite (Mucci and Morse, 1983). Evans et al. (2015) hypothesize that the incorporation of other alkali elements, like Na is also related, due to lattice distortion by the incorporation of Mg, which has been found in inorganic calcite (Okumura and Kitano, 1986). However, although this mechanism might explain some of the observed species specific element incorporation in hyaline foraminifera, this does not explain the observed difference between hyaline and porcelaneous foraminifera (Figure 4). Porcelaneous foraminifera have generally high Mg/Ca, but we actually observe lower incorporation of Na and Sr compared to hyaline species with similar D_{Mg} (Fig 4, upper right and left panel: D_{Mg} versus D_{Na} and D_{Sr}). When including porcelaneous species from other studies we also observe no increase in D_{Sr} over a larger range in D_{Mg} (Fig S1, upper left panel: D_{Mg} versus D_{Sr}). Therefore, even though this interdependence might partly stem from mechanisms associated with crystallography, differences between hyaline and porcelaneous foraminifera suggest it could also be caused by mechanisms involved in take up the ions (Ca^{2+} and CO_3^{2-}) necessary for chamber formation, which are different for hyaline and porcelaneous species, reflected in the different trends observed here.

4.4. Ion transport models

Both porcelaneous and hyaline foraminifera promote calcification by increasing their internal pH (De Nooijer et al., 2009). Still, they might use different mechanisms to take up the ions (Ca^{2+} and CO_3^{2-})

necessary for chamber formation, which is reflected in the different trends observed here. In both porcelaneous and hyaline foraminifera, E/Ca respond similarly to changes in pCO_2 (Fig 3), suggesting uptake of all these elements is controlled by the same process. However, we observed different inter-element relations between hyaline and porcelaneous foraminifera (Fig. 4), indicating the mechanisms for ion transport might be different for these two groups. Two of the main concepts of ion transport in foraminifera are transmembrane transport (Nehrke et al., 2013) and the inclusion of seawater by seawater endocytosis (Bentov et al., 2009). Here we try to validate these two concept by comparing them with our observations.

4.4.1. Transmembrane transport

During calcification, Ca^{2+} is proposed to be transported from seawater to the SOC via ion channels (Nehrke et al., 2013), likely in exchange for protons (Toyofuku et al., accepted). This so-called trans-membrane transport (TMT) through Ca^{2+} channels has also been found for other marine organisms, including coccolithophores (Gussone et al., 2006). These Ca^{2+} channels may not discriminate perfectly between Ca ions and elements like Mg, Sr, Ba, Na (Sather, 2005; Allen and Sanders, 1994; Hess and Tsien, 1984), causing accidental transport of these elements into the SOC. How much of a certain element will enter the SOC in this way, depends on 1) the selectiveness of the channels and the characteristics of the transported ions (like atomic radius), 2) the element to calcium ratio in the foraminiferal microenvironment and 3) the concentration gradient between seawater and the SOC. The availability of some free ions, like Ba and Zn, changes as a function of pCO_2 due to the formation of carbonate complexes (Fig. 5). When Zn and Ba form stable complexes with carbonate ions they are no longer available for (sporadic) transport through the Ca^{2+} channels, decreasing the availability at the site of calcification and subsequently, incorporation into the foraminiferal calcite. Thus, transmembrane transport of ions by Ca^{2+} to the SOC is in agreement with our results (Fig. 3). The amount of Zn and Ba available at the site of calcification is proportional to the concentration of the ratio between Ca^{2+} and free Zn^{2+} and Ba^{2+} in the foraminiferal microenvironment. In turn, the amount of free Zn and Ba ions in seawater is controlled by their respective concentration in seawater concentration, as well as carbonate

chemistry (Fig 5). Foraminiferal Mg/Ca, Na/Ca and Sr/Ca is not detectably affected, since the availability of Mg^{2+}, Na^{+} and Sr^{2+} does not change over the range of $[CO_3^{2-}]$ studied here. However, the large range in Mg/Ca values in hyaline species suggests that TMT might play a variable role in the calcification process of these species. This may result in an interdependence between all these elements studied such as observed here for the hyaline species if the selectivity for Ca^{2+} of these channels varies between species.

4.4.2. Seawater endocytosis

Another proposed ion transport mechanism is seawater endocytosis (Bentov et al., 2009; Erez, 2003), in which seawater is vacuolized, altered and then used as a calcifying fluid. The chemistry or elemental composition of the vacuolized seawater or the calcification fluid is in this case depending on the seawater concentration. Inter-species differences would therefore be minimized, as is observed for porcelaneous foraminifera in our study (Fig. 4). However, this concept cannot explain the overserved changes in Zn/Ca and Ba/Ca as a function of pCO_2, which are caused by the speciation of elements in seawater due to changes in the carbonate chemistry (Fig. 5). The concentration of total e.g. Zn in the seawater vacuoles does not change for the different treatments, only the species of Zn present. Only if the internal pH in the vacuole depends on ambient seawater pH, which is currently unknown, there is a potential for changes in speciation. In theory, if pH will change in concert with ambient seawater, such a change in internal pH from >9 (De Nooijer et al., 2009) to >8.6 (ΔpH = 0.4 in our treatment) changes $[CO_3^{2-}]$ and thus the speciation of e.g. Zn (and Ba) at the site of calcification. However, over this range the change in $[CO_3^{2-}]$ will be rather limited and hence such an effect of differential speciation within the calcifying fluid does not suffice to explain the observed sensitivity of Zn and Ba to pCO_2 in our study. This is in line with recent evidence on Zn/Ca in foraminifera, which suggests Zn incorporation is not primarily governed by changes in seawater pH, but by carbonate ion concentration, which does not change much at these high pH's (van Dijk et al., 2017).

4.5. Consequences for calcification in hyaline and porcelaneous species

Both ion transport mechanisms, and their consequences for Zn and Ba incorporation, are summarized in Fig. 6. The observed species-specific element incorporation in hyaline foraminifera (Fig. 4) is compatible with the transmembrane transport mixing model proposed by Nehrke et al. (2013), where species specific differences in E/Ca are explain by the relative contribution of transmembrane transport and so-called passive transport. In contrast to hyaline species, the porcelaneous species show much less inter-species variation in element composition (Fig. 3), suggesting that this group of foraminifera calcify from a fluid comparable to ambient seawater (Ter Kuile and Erez, 1987), by e.g. seawater endocytosis (Fig. 6, panel B) with only minor alteration of the elemental composition of the calcifying fluid by ion channels. However, the observed correlation between pCO_2 and Ba and Zn (Fig. 3) suggests that Ca channels still play a (modest) role in supplying Ca^{2+} to the porcelaneous SOC, since possible speciation of minor and trace elements in the SOC caused by a change in the internal pH is probably not sufficient to explain observed patterns (4.4.2). However since porcelaneous species already obtain calcium by including seawater in their calcification vesicle prior to calcite precipitation, contribution of Ca^{2+} through TMT is likely smaller than in hyaline species, which may explain the observed lower sensitivity of e.g. foraminiferal Zn/Ca and Ba/Ca to changes in seawater [CO_3^{2-}] in porcelaneous species (Fig. 3). This approximately 2 times lower sensitivity of porcelaneous foraminifera compared to hyaline species suggests that porcelaneous foraminifera acquire half of the necessary Ca^{2+} through Ca-channels compared to hyaline species. Element incorporation in porcelaneous foraminifera will therefore be mainly governed by their respective concentrations in seawater, and to a lesser extent by the selectivity for Ca^{2+}/permeability for other ions during TMT.

5. Conclusions

Trends in element incorporation in larger benthic foraminifera can be explained by a combination of differences in calcification strategy and seawater chemistry. Carbonate chemistry of seawater determines speciation and therefore availability of some ions (e.g. Zn^{2+} and Ba^{2+}), which are available

for ion transport to the site of calcification. For hyaline foraminifera, we observed species-specific interdependence of element incorporation, which can be explained by a previously proposed transmembrane transport model and the bioavailability of ions in seawater during calcification. For porcelaneous foraminifera, species specific difference are small, hinting at a higher contribution of another ion source, like e.g. seawater endocytosis.

Acknowledgments

This research is funded by the NIOZ – Royal Netherlands Institute for Sea Research and the Darwin Centre for Biogeosciences project "*Double Trouble*: Consequences of Ocean Acidification – Past, Present and Future –Evolutionary changes in calcification mechanisms" and the program of the Netherlands Earth System Science Center (NESSC). We would like to thanks both reviewers, Dr. David Evans and Dr. Kazuhiko Fujita for their constructive comments. Great thanks to Johan Stapel for hosting the 2015 foraminifera culture expedition at the CNSI, St. Eustatius, as well as all the participants: Jelle Bijma and Gernot Nehrke (AWI), Brett Metcalfe (VU), Alice Webb (NIOZ), Esmee Geerken (NIOZ) and Didier de Bakker (NIOZ/IMARES). This study would not have been possible without Steven van Heuven and Bob Koster, who designed and constructed the pCO_2 set-up (NWO grants 858.14.021 and 858.14.022). Furthermore, we would like to thank Kirsten Kooijman for supplying *Dunaliella salina* cultures, Patrick Laan and Karel Bakker for seawater analysis and Mariëtte Wolthers for providing technical support with PHREEQC. Lastly, we thank Jan-Berend Stuut (NIOZ) for the usage of the Hitachi TM3000 SEM (NWO grant 822.01.008 and ERC grant 311152).

References

Allen, G. J., and Sanders, D.: Two Voltage-Gated, Calcium Release Channels Coreside in the Vacuolar Membrane of Broad Bean Guard Cells, The Plant Cell, 6, 685-694, 10.1105/tpc.6.5.685, 1994.

Allison, N., Austin, H., Austin, W., and Paterson, D. M.: Effects of seawater pH and calcification rate on test Mg/Ca and Sr/Ca in cultured individuals of the benthic, calcitic foraminifera *Elphidium williamsoni*, Chemical Geology, 289, 171-178, 10.1016/j.chemgeo.2011.08.001, 2011.

Angell, R. W.: Test morphogenesis (chamber formation) in the foraminifer *Spiroloculina hyalina* Schulze, Journal of Foraminiferal Research, 10, 89-101, 1980.

Barker, S., Higgins, J. A., and Elderfield, H.: The future of the carbon cycle: review, calcification response, ballast and feedback on atmospheric CO_2, Philos Trans A Math Phys Eng Sci, 361, 1977-1998; discussion 1998-1979, 10.1098/rsta.2003.1238, 2003.

Bentov, S., and Erez, J.: Impact of biomineralization processes on the Mg content of foraminiferal shells: A biological perspective, Geochemistry, Geophysics, Geosystems, 7, 2006.

Bentov, S., Brownlee, C., and Erez, J.: The role of seawater endocytosis in the biomineralization process in calcareous foraminifera, Proceedings of the National Academy of Sciences of the United States of America, 106, 21500-21504, 10.1073/pnas.0906636106, 2009.

Bernhard, J. M., Blanks, J. K., Hintz, C. J., and Chandler, G. T.: Use of the fluorescent calcite marker calcein to label foraminiferal tests, Journal of Foraminiferal Research, 34, 96-101, 10.2113/0340096, 2004.

Berthold, W.-U.: Biomineralisation bei milioliden Foraminiferen und die Matritzen-Hypothese, Naturwissenschaften, 63, 196-197, 1976.

De Nooijer, L. J., Toyofuku, T., and Kitazato, H.: Foraminifera promote calcification by elevating their intracellular pH, Proceedings of the National Academy of Sciences, 106, 15374-15378, 10.1073/pnas.0904306106, 2009.

De Nooijer, L. J., Spero, H. J., Erez, J., Bijma, J., and Reichart, G. J.: Biomineralization in perforate foraminifera, Earth-Science Reviews, 135, 48-58, http://dx.doi.org/10.1016/j.earscirev.2014.03.013, 2014.

Debenay, J.-P., Guillou, J.-J., Geslin, E., Lesourd, M., and Redois, F.: Processus de cristallisation de plaquettes rhomboédriques à la surface d'un test porcelané de foraminifère actuel, Geobios, 31, 295-302, 1998.

Dickson, A. G.: Thermodynamics of the dissociation of boric acid in synthetic seawater from 273.15 to 318.15 K, Deep Sea Research Part A. Oceanographic Research Papers, 37, 755-766, http://dx.doi.org/10.1016/0198-0149(90)90004-F, 1990.

Dissard, D., Nehrke, G., Reichart, G. J., Nouet, J., and Bijma, J.: Effect of the fluorescent indicator calcein on Mg and Sr incorporation into foraminiferal calcite, Geochemistry, Geophysics, Geosystems, 10, 10.1029/2009GC002417, 2009.

Dissard, D., Nehrke, G., Reichart, G. J., and Bijma, J.: Impact of seawater pCO_2 on calcification and Mg/Ca and Sr/Ca ratios in benthic foraminifera calcite: results from culturing experiments with *Ammonia tepida*, Biogeosciences, 7, 81-93, 10.5194/bg-7-81-2010, 2010.

Dueñas-Bohórquez, A., Raitzsch, M., De Nooijer, L. J., and Reichart, G.-J.: Independent impacts of calcium and carbonate ion concentration on Mg and Sr incorporation in cultured benthic foraminifera, Marine Micropaleontology, 81, 122-130, 10.1016/j.marmicro.2011.08.002, 2011.

Elderfield, H., Bertram, C. J., and Erez, J.: A biomineralization model for the incorporation of trace elements into foraminiferal calcium carbonate, Earth and Planetary Science Letters, 142, 409-423, http://dx.doi.org/10.1016/0012-821X(96)00105-7, 1996.

456 Elderfield, H., and Ganssen, G.: Past temperature and $\delta^{18}O$ of surface ocean waters inferred
457 from foraminiferal Mg/Ca ratios, Nature, 405, 442-445, 2000.
458 Elderfield, H., Yu, J., Anand, P., Kiefer, T., and Nyland, B.: Calibrations for benthic
459 foraminiferal Mg/Ca paleothermometry and the carbonate ion hypothesis, Earth and Planetary
460 Science Letters, 250, 633-649, 2006.
461 Erez, J.: The source of ions for biomineralization in foraminifera and their implications for
462 paleoceanographic proxies, Reviews in Mineralogy and Geochemistry, 54, 115-149,
463 10.2113/0540115, 2003.
464 Evans, D., Erez, J., Oron, S., and Müller, W.: Mg/Ca-temperature and seawater-test
465 chemistry relationships in the shallow-dwelling large benthic foraminifera *Operculina*
466 *ammonoides*, Geochimica et Cosmochimica Acta, 148, 325-342, 2015.
467 Evans, D., Wade, B. S., Henehan, M., Erez, J., and Müller, W.: Revisiting carbonate
468 chemistry controls on planktic foraminifera Mg /Ca: implications for sea surface temperature
469 and hydrology shifts over the Paleocene–Eocene Thermal Maximum and Eocene–Oligocene
470 transition, Clim. Past, 12, 819-835, 10.5194/cp-12-819-2016, 2016.
471 Guillong, M., Meier, D. L., Allan, M. M., Heinrich, C. A., and Yardley, B. W.: SILLS: A
472 MATLAB-based program for the reduction of laser ablation ICP-MS data of homogeneous
473 materials and inclusions, Mineralogical Association of Canada Short Course Series, 40, 328-
474 333, 2008.
475 Gussone, N., Langer, G., Thoms, S., Nehrke, G., Eisenhauer, A., Riebesell, U., and Wefer,
476 G.: Cellular calcium pathways and isotope fractionation in *Emiliania huxleyi*, Geology, 34, 625-
477 628, 2006.
478 Hemleben, C., Be, A. W. H., Anderson, O. R., and Tuntivate, S.: Test morphology, organic
479 layers and chamber formation of the planktonic foraminifer *Globorotalia menardii* (d'Orbigny),
480 Journal of Foraminiferal Research, 7, 1-25, 10.2113/gsjfr.7.1.1, 1977.

Hemleben, C., Erson, O., Berthold, W., and Spindler, M.: fout, Biomineralization in lower plants and animals (BSC Leadbeater, R Riding, eds) Clarendon Press, Oxford, 237-249, 1986.

Hess, P., and Tsien, R. W.: Mechanism of ion permeation through calcium channels, Nature, 309, 453-456, 1984.

Hönisch, B., Allen, K. A., Russell, A. D., Eggins, S. M., Bijma, J., Spero, H. J., Lea, D. W., and Yu, J.: Planktic foraminifers as recorders of seawater Ba/Ca, Marine Micropaleontology, 79, 52-57, 2011.

Jochum, K. P., Scholz, D., Stoll, B., Weis, U., Wilson, S. A., Yang, Q., Schwalb, A., Börner, N., Jacob, D. E., and Andreae, M. O.: Accurate trace element analysis of speleothems and biogenic calcium carbonates by LA-ICP-MS, Chemical Geology, 318–319, 31-44, http://dx.doi.org/10.1016/j.chemgeo.2012.05.009, 2012.

Keul, N., Langer, G., De Nooijer, L. J., Nehrke, G., Reichart, G.-J., and Bijma, J.: Incorporation of uranium in benthic foraminiferal calcite reflects seawater carbonate ion concentration, Geochemistry, Geophysics, Geosystems, 14, 102-111, 10.1029/2012gc004330, 2013.

Kurtarkar, S. R., Saraswat, R., Nigam, R., Banerjee, B., Mallick, R., Naik, D. K., and Singh, D. P.: Assessing the effect of calcein incorporation on physiological processes of benthic foraminifera, Marine Micropaleontology, 114, 36-45, http://dx.doi.org/10.1016/j.marmicro.2014.10.001, 2015.

Langer, G., Sadekov, A., Thoms, S., Keul, N., Nehrke, G., Mewes, A., Greaves, M., Misra, S., Reichart, G.-J., de Nooijer, L. J., Bijma, J., and Elderfield, H.: Sr partitioning in the benthic foraminifera Ammonia aomoriensis and Amphistegina lessonii, Chemical Geology, 440, 306-312, http://dx.doi.org/10.1016/j.chemgeo.2016.07.018, 2016.

Lea, D. W., Mashiotta, T. A., and Spero, H. J.: Controls on magnesium and strontium uptake in planktonic foraminifera determined by live culturing, Geochimica et Cosmochimica Acta, 63, 2369-2379, http://dx.doi.org/10.1016/S0016-7037(99)00197-0, 1999.

Lear, C. H., Elderfield, H., and Wilson, P. A.: Cenozoic deep-Sea temperatures and global ice volumes from Mg/Ca in benthic foraminiferal calcite, Science, 287, 269-272, 10.1126/science.287.5451.269, 2000.

Lueker, T. J., Dickson, A. G., and Keeling, C. D.: Ocean pCO2 calculated from dissolved inorganic carbon, alkalinity, and equations for K1 and K2: validation based on laboratory measurements of CO2 in gas and seawater at equilibrium, Marine Chemistry, 70, 105-119, http://dx.doi.org/10.1016/S0304-4203(00)00022-0, 2000.

Marchitto, T. M., Curry, W. B., and Oppo, D. W.: Zinc concentrations in benthic foraminifera reflect seawater chemistry, Paleoceanography, 15, 299-306, 10.1029/1999PA000420, 2000.

Marchitto, T. M., Lynch-Stieglitz, J., and Hemming, S. R.: Deep Pacific $CaCO_3$ compensation and glacial–interglacial atmospheric CO_2, Earth and Planetary Science Letters, 231, 317-336, http://dx.doi.org/10.1016/j.epsl.2004.12.024, 2005.

McCorkle, D. C., Martin, P. A., Lea, D. W., and Klinkhammer, G. P.: Evidence of a dissolution effect on benthic foraminiferal shell chemistry: $\delta^{13}C$, Cd/Ca, Ba/Ca, and Sr/Ca results from the Ontong Java Plateau, Paleoceanography, 10, 699-714, 10.1029/95PA01427, 1995.

Mewes, A., Langer, G., Reichart, G.-J., De Nooijer, L. J., Nehrke, G., and Bijma, J.: The impact of Mg contents on Sr partitioning in benthic foraminifers, Chemical Geology, 412, 92-98, http://dx.doi.org/10.1016/j.chemgeo.2015.06.026, 2015.

Mezger, E. M., de Nooijer, L. J., Boer, W., Brummer, G. J. A., and Reichart, G. J.: Salinity controls on Na incorporation in Red Sea planktonic foraminifera, Paleoceanography, 10.1002/2016PA003052, 2016.

Mucci, A., and Morse, J. W.: The incorporation of Mg^{2+} and Sr^{2+} into calcite overgrowths: influences of growth rate and solution composition, Geochimica et Cosmochimica Acta, 47, 217-233, http://dx.doi.org/10.1016/0016-7037(83)90135-7, 1983.

Nardelli, M. P., Malferrari, D., Ferretti, A., Bartolini, A., Sabbatini, A., and Negri, A.: Zinc incorporation in the miliolid foraminifer Pseudotriloculina rotunda under laboratory conditions, Marine Micropaleontology, 126, 42-49, http://dx.doi.org/10.1016/j.marmicro.2016.06.001, 2016.

Nehrke, G., Keul, N., Langer, G., De Nooijer, L. J., Bijma, J., and Meibom, A.: A new model for biomineralization and trace - element signatures of Foraminifera tests, Biogeosciences, 10, 6759-6767, 10.5194/bg-10-6759-2013, 2013.

Nürnberg, D., Bijma, J., and Hemleben, C.: Assessing the reliability of magnesium in foraminiferal calcite as a proxy for water mass temperatures, Geochimica et Cosmochimica Acta, 60, 803-814, 10.1016/0016-7037(95)00446-7, 1996.

Okai, T., Suzuki, A., Kawahata, H., Terashima, S., and Imai, N.: Preparation of a New Geological Survey of Japan Geochemical Reference Material: Coral JCp-1, Geostandards newsletter, 26, 95-99, 2002.

Okumura, M., and Kitano, Y.: Coprecipitation of alkali metal ions with calcium carbonate, Geochimica et Cosmochimica Acta, 50, 49-58, http://dx.doi.org/10.1016/0016-7037(86)90047-5, 1986.

Parkhurst, D. L., and Appelo, C.: User's guide to PHREEQC (Version 2): A computer program for speciation, batch-reaction, one-dimensional transport, and inverse geochemical calculations, US Geol. Surv, Denver, Colorado, 1999.

552 Pawlowski, J., Holzmann, M., Berney, C., Fahrni, J., Gooday, A. J., Cedhagen, T., Habura,
553 A., and Bowser, S. S.: The evolution of early Foraminifera, Proc Natl Acad Sci U S A, 100,
554 11494-11498, 10.1073/pnas.2035132100, 2003.
555 Pierrot, D., Lewis, E., and Wallace, D. W. R.: MS Excel Program Developed for CO_2 System
556 Calculations, Carbon Dioxide Information Analysis Center, Oak Ridge National Laboratory,
557 U.S., 2006.
558 Reichart, G.-J., Jorissen, F., Anschutz, P., and Mason, P. R.: Single foraminiferal test
559 chemistry records the marine environment, Geology, 31, 355-358, 2003.
560 Russell, A. D., Hönisch, B., Spero, H. J., and Lea, D. W.: Effects of seawater carbonate ion
561 concentration and temperature on shell U, Mg, and Sr in cultured planktonic foraminifera,
562 Geochimica et Cosmochimica Acta, 68, 4347-4361, 10.1016/j.gca.2004.03.013, 2004.
563 Sanyal, A., Hemming, N. G., Broecker, W. S., Lea, D. W., Spero, H. J., and Hanson, G. N.:
564 Oceanic pH control on the boron isotopic composition of foraminifera: Evidence from culture
565 experiments, Paleoceanography, 11, 513-517, 1996.
566 Sather, W. A.: Selective Permeability of Voltage-Gated Calcium Channels, in: Voltage-
567 Gated Calcium Channels, Springer US, Boston, MA, 205-218, 2005.
568 Segev, E., and Erez, J.: Effect of Mg/Ca ratio in seawater on shell composition in shallow
569 benthic foraminifera, Geochemistry, Geophysics, Geosystems, 7, 10.1029/2005GC000969,
570 2006.
571 Ter Kuile, B., and Erez, J.: Uptake of inorganic carbon and internal carbon cycling in
572 symbiont-bearing benthonic foraminifera, Marine Biology, 94, 499-509, 1987.
573 Toyofuku, T., Suzuki, M., Suga, H., Sakai, S., Suzuki, A., Ishikawa, T., De Nooijer, L. J.,
574 Schiebel, R., Kawahata, H., and Kitazato, H.: Mg/Ca and $\delta^{18}O$ in the brackish shallow-water
575 benthic foraminifer *Ammonia 'beccarii'*, Marine Micropaleontology, 78, 113-120,
576 http://dx.doi.org/10.1016/j.marmicro.2010.11.003, 2011.

Toyofuku, T., Matsuo, M. Y., de Nooijer, L. J., Nagai, Y., Kawada, S., Fujita, K., Reichart, G.-J., Nomaki, H., Tsuchiya, M., Sakaguchi, H., and Kitazato, H.: Proton pumping accompanies calcification in foraminifera, Nature Communications, accepted.

van Dijk, I., de Nooijer, L. J., Wolthers, M., and Reichart, G.-J.: Impacts of pH and [CO_3^{2-}] on the incorporation of Zn in foraminiferal calcite, Geochimica et Cosmochimica Acta, 197, 263-277, http://dx.doi.org/10.1016/j.gca.2016.10.031, 2017.

Wit, J. C., De Nooijer, L. J., Barras, C., Jorissen, F. J., and Reichart, G. J.: A reappraisal of the vital effect in cultured benthic foraminifer *Bulimina marginata* on Mg/Ca values: assessing temperature uncertainty relationships, Biogeosciences, 9, 3693-3704, 10.5194/bg-9-3693-2012, 2012.

Wit, J. C., De Nooijer, L. J., Wolthers, M., and Reichart, G. J.: A novel salinity proxy based on Na incorporation into foraminiferal calcite, Biogeosciences, 10, 6375-6387, 10.5194/bg-10-6375-2013, 2013.

Yu, J., and Elderfield, H.: Benthic foraminiferal B/Ca ratios reflect deep water carbonate saturation state, Earth and Planetary Science Letters, 258, 73-86, 10.1016/j.epsl.2007.03.025, 2007.

Zeebe, R. E., and Sanyal, A.: Comparison of two potential strategies of planktonic foraminifera for house building: Mg^{2+} or H^+ removal?, Geochimica et Cosmochimica Acta, 66, 1159-1169, http://dx.doi.org/10.1016/S0016-7037(01)00852-3, 2002.

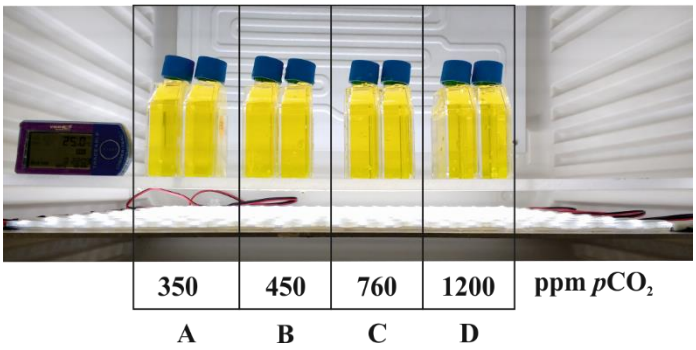

596

597 **Figure 1. Photograph of the culture set-up. Four duplicate bottles with culture media (with**
598 **calcein added) and adult specimens of foraminifera. Treatment with corresponding set-points**
599 **are A=350 ppm, B=450 ppm, C=760 ppm, D=1200 ppm CO_2.**

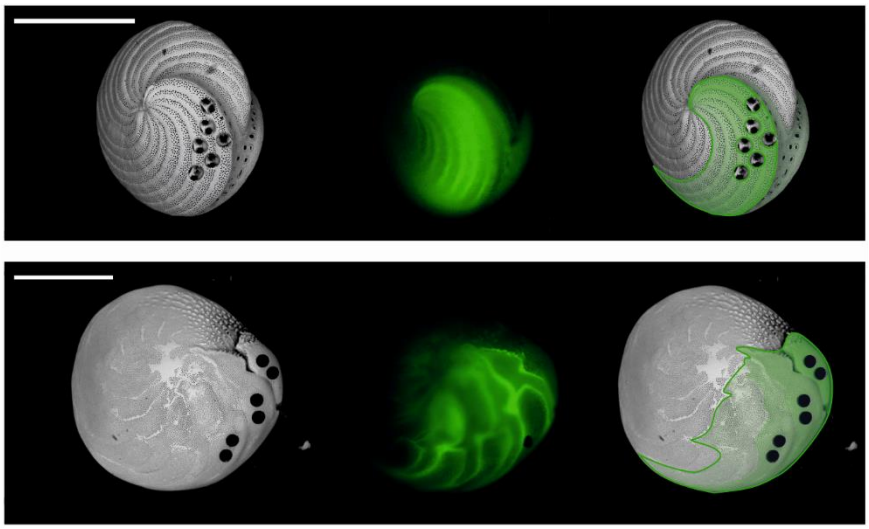

Figure 2. SEM (left) and fluorescence microscope (middle) photographs of *A. angulatus* (top series) and *A. gibbosa* (bottom series) to assess newly formed chambers for laser ablation (right). Scale bar = 500 µm.

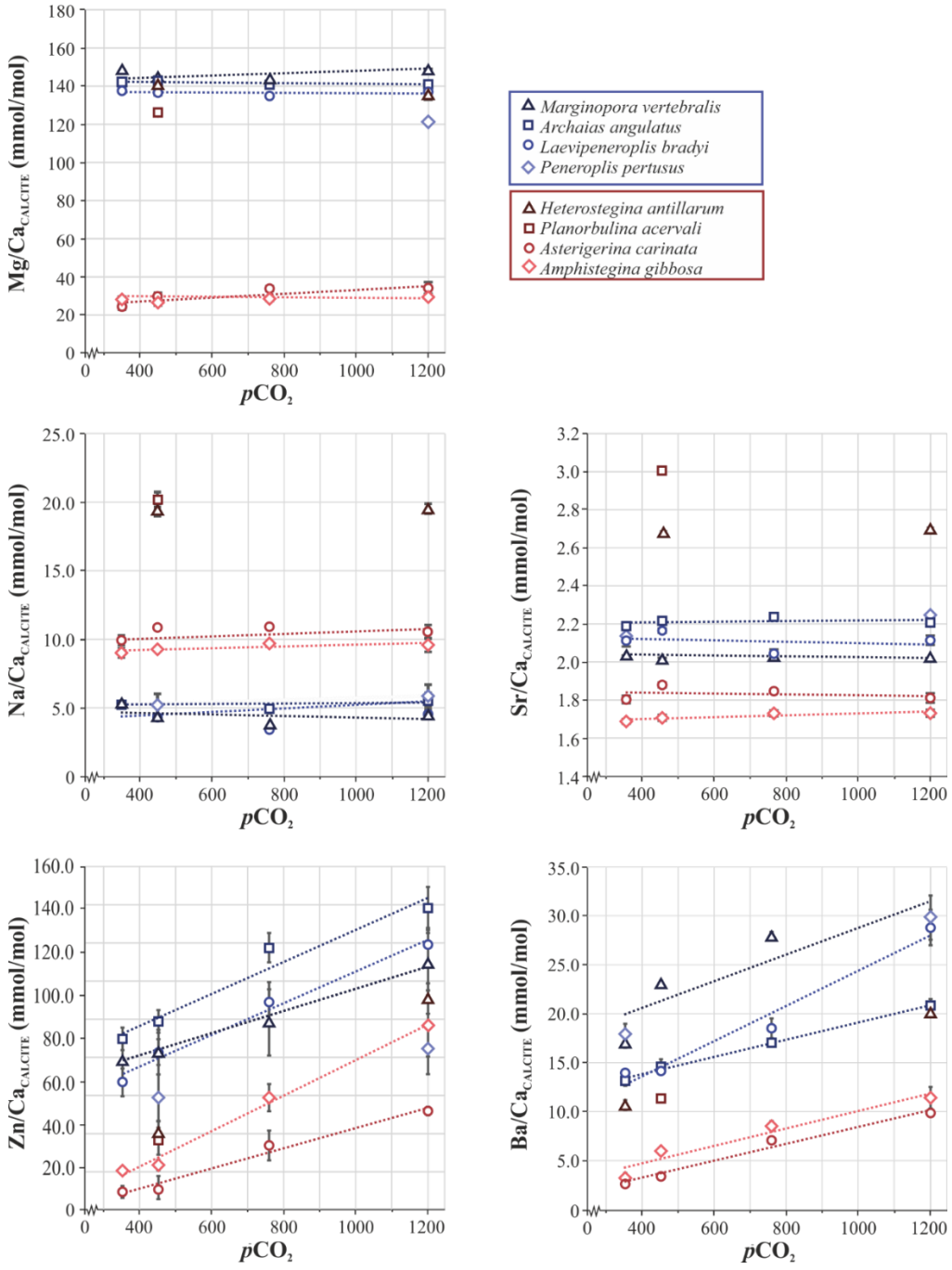

Figure 3. Element to Ca ratios (±SE) of different species of foraminifera over a range of pCO_2 values. In some cases, the error bar is smaller than the symbol. Porcelaneous species in blue (triangles = *S. marginalis*; squares = *A. angulatus*; circles = *L. bradyi*; squares = *P. pertusus*) and hyaline species in red (triangles = *H. antillarum*; squares = *P. acervalis*; circles = A. *carinata;* diamonds = *A. gibbosa*).

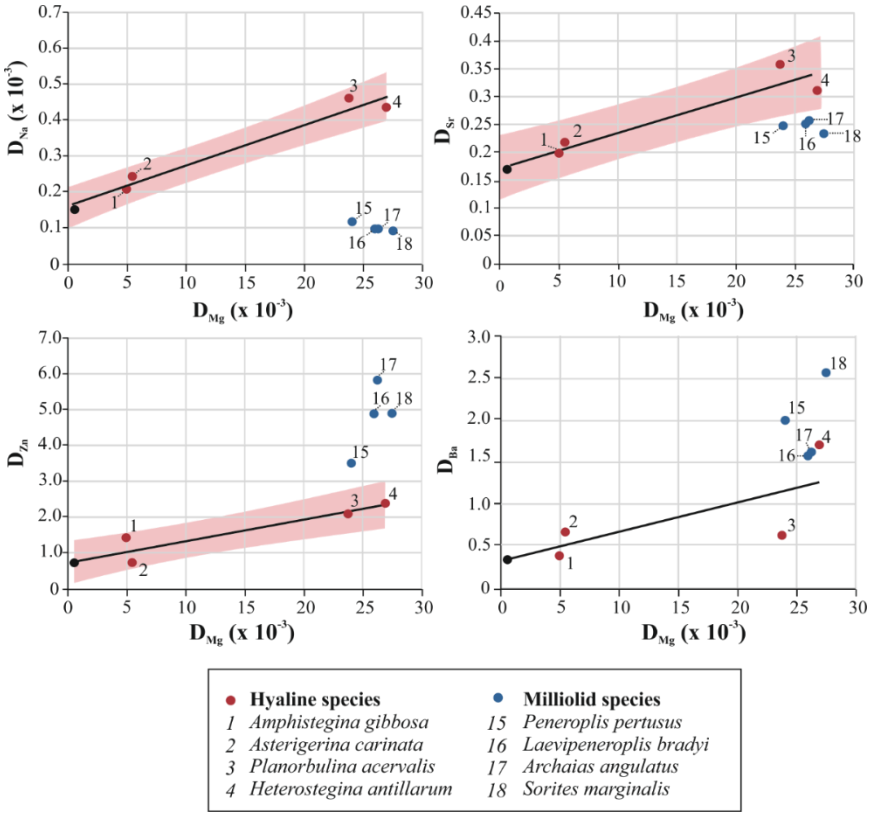

610

611 **Figure 4. Partition coefficient of Na, Sr, Zn and Ba versus D_{Mg} of hyaline (red symbols) and**
612 **porcelaneous (blue symbols) species. Black lines represent linear trendlines. The 95% confidence**
613 **intervals of signification trends ($p<0.025$) are indicated in red. Black dots represent the NFHS, in-**
614 **house carbonate standard, consisting of planktonic foraminifera. Numbers correspond to**
615 **foraminiferal species analyzed, numbers 5-14 and 18-21 represent values from previously**
616 **published species and are included in Figure S1 (supplementary information).**

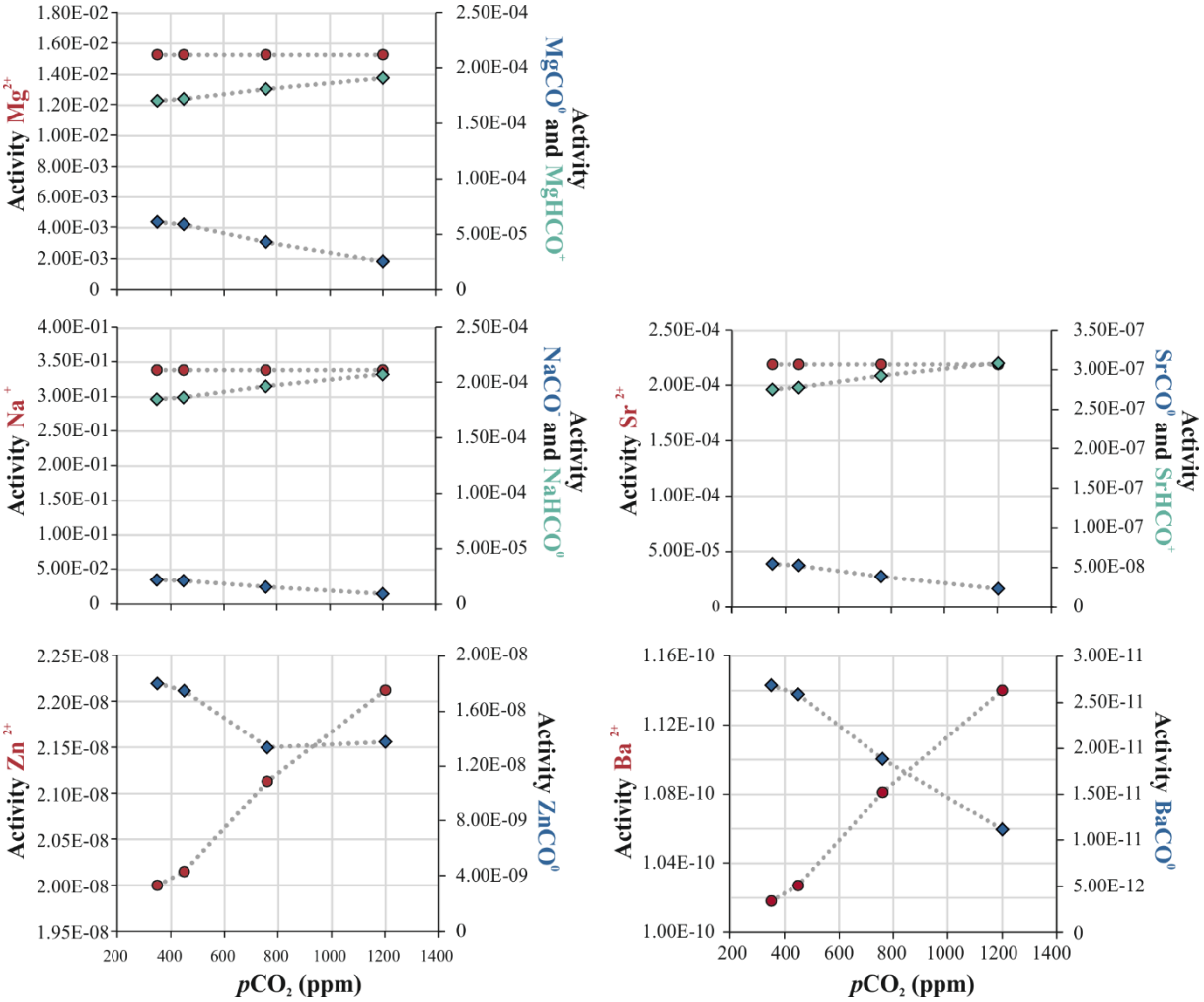

Figure 5. Speciation of Mg, Na, Sr, Zn and Ba in the different seawater treatments modelled in PHREEQC (Parkhurst and Appelo, 1999). Activities of free ions (red) and element (E)-carbonate complexes (ECO_3 = blue diamonds and $EHCO_3$ = green diamonds).

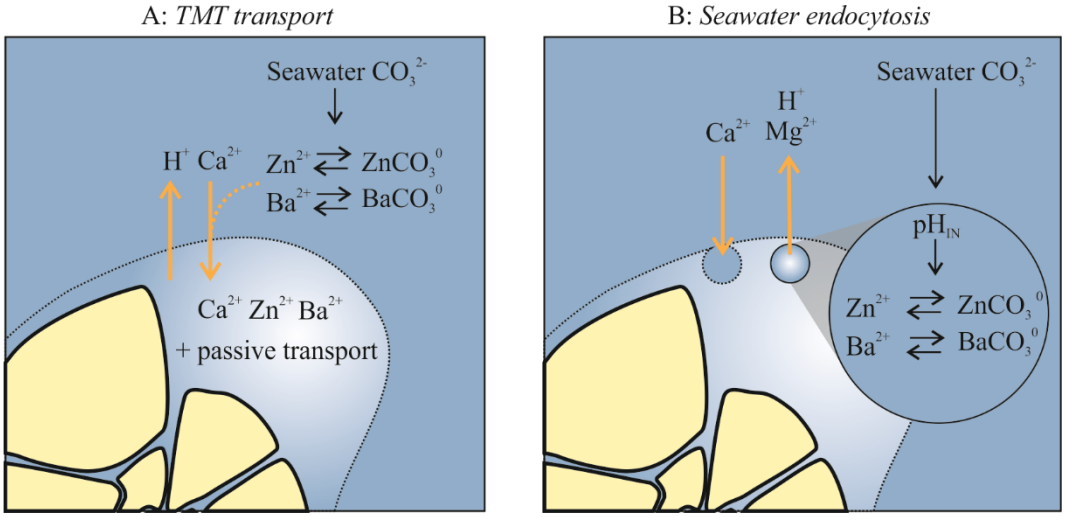

621

622 **Figure 6. Schematic overview of different mechanisms for ion transport during foraminiferal**
623 **calcification. Orange arrows indicate transport of ions. A) The transmembrane transport (TMT)**
624 **mixing model as proposed by Nehrke et al. (2013). The amount of free ions, e.g. Zn^{2+} and Ba^{2+},**
625 **available for transport by Ca^{2+} in exchange for protons (Toyofuku et al., accepted) is influenced**
626 **by speciation due to changes in seawater [CO_3^{2-}]. The composition of the seawater at the site of**
627 **calcification is determined by both TMT and passive transport B) Simplified overview of seawater**
628 **endocytosis (Bentov et al., 2009; Erez, 2003), were speciation of Zn^{2+} and Ba^{2+} is determined by**
629 **changes in internal pH (pH_{IN}), which changes with ambient seawater carbonate chemistry. Based**
630 **on our observations, panel A likely applies to hyaline species, whereas panel B represents**
631 **porcelaneous calcification.**

Treatment	Set-point	Measured		Calculated CO2SYS		
	pCO_2 ppm	TA µmol/kg	DIC µmol/kg	$[CO_3^{2-}]$ µmol/kg	pH (total scale)	$\Omega_{CALCITE}$
A	350	2302.8±8.2	2007.5±10.7	220.7	8.06	5.4
B	450	2305.2±5.8	2021.3±12.5	200.0	8.01	4.9
C	760	2304.4±0.9	2100.8±13.4	153.7	7.87	3.7
D	1200	2300.3±0.7	2201.4±4.1	92.2	7.61	2.2

Table 1. Carbon parameters (TA= Total alkalinity, n=2, DIC=Dissolved Inorganic Carbon, n=2) with (relative) standard deviation of the culture water per treatment of the pCO_2 experiment. CO2SYS was used to calculate seawater carbonate ion concentration, calcite saturation state and pH from measured TA and DIC.

Species	n measurements (n specimens)			
	A: 350 ppm	B: 450ppm	C:760 ppm	D:1200 ppm
A. angulatus	62 (19)	72 (21)	76 (21)	51 (14)
S. marginalis	48 (14)	49 (15)	57 (18)	33 (11)
A. gibbosa	106 (28)	126 (32)	75 (18)	59 (15)
L. bradyi	21 (5)	38 (13)	27 (5)	16 (4)
A. carinata	12 (2)	14 (1)	19 (4)	5 (1)
P. pertusus		12 (2)		11 (2)
H. antillarum		12 (1)		14 (2)
P. acervalis		8 (2)		
Total	187 (49)	331 (87)	254 (66)	189 (49)

636 **Table 2. Total number of LA-ICP-MS measurements per species, per treatment (A-D).**

Species	pCO_2	Mg/Ca mmol/mol		Na/Ca mmol/mol		Sr/Ca mmol/mol		Zn/Ca µmol/mol		Ba/Ca µmol/mol	
		Avg±SE	D_{Mg} $*10^{-3}$	Avg±SE	D_{Na} $*10^{-3}$	Avg±SE	D_{Sr}	Avg±SE	D_{Zn}	Avg±SE	D_{Ba}
Porcelaneous species											
A. angulatus	350	139.4±0.6$_a$	26.6	5.2±0.1^a	0.12	2.2±0.02^a	0.25	80.0±5.1^a	5.3	13.2±0.5^a	1.5
	450	137.7±0.5$_b$	26.3	4.3±0.1^b	0.10	2.2±0.01^a	0.26	88.1±5.2^b	5.8	14.6±0.5^b	1.6
	760	137.4±0.7$_b$	26.2	4.9±0.1^c	0.11	2.2±0.01^a	0.26	122.6±7.0^c	8.1	17.0±0.6^b	1.9
	1200	138.6±1.1^a	26.4	5.4±0.2^a	0.12	2.2±0.02^a	0.26	140.8±9.9^d	9.3	20.9±0.2^c	2.3
S. marginalis	350	147.7±0.6^a	28.2	4.8±0.1^a	0.11	2.0±0.01^a	0.24	70.0±10.1^a	4.6	17.0±0.5^a	1.9
	450	144.2±0.8^b	27.5	4.1±0.1^b	0.09	2.0±0.01^a	0.23	74.0±10.6^b	4.9	23.1±0.5^b	2.6
	760	143.0±0.6^a	27.3	3.8±0.1^a	0.09	2.0±0.01^a	0.23	87.7±15.5^c	5.8	27.9±0.6^c	3.1
	1200	148.3±0.5^b	28.3	4.5±0.2^c	0.10	2.0±0.01^a	0.23	115.6±15.3^d	7.6	30.1±0.2^d	3.3
L. bradyi	350	137.8±1.3^a	26.3	5.2±0.2^c	0.12	2.1±0.03^a	0.24	60.0±6.5^a	4.0	14.0±0.5^a	1.5
	450	136.2±0.7^a	26.0	4.3±0.1^b	0.10	2.2±0.01^b	0.25	73.8±6.0^b	4.9	14.2±0.5^a	1.6
	760	134.4±1.2^b	25.6	3.4±0.1^a	0.08	2.0±0.02^c	0.24	97.5±9.4^c	6.4	18.5±0.6^b	2.1
	1200	136.9±1.1^a	26.1	6.2±0.2^d	0.14	2.1±0.02^a	0.24	124.2±7.8^d	8.2	28.8±0.2^c	3.2
P. pertusus	350										
	450	126.1±1.8^a	24.0	5.2±0.3^a	0.12	2.1±0.07^a	0.25	53.0±10.8^a	3.5	18.0±0.5^a	2.0
	760										
	1200	121.3±1.0^a	23.1	5.8±0.2^a	0.13	2.2±0.02^a	0.26	75.5±11.9^b	5.0	29.8±0.2^b	3.3

Hyaline species											
H. antillarum	350										
	450	141.3±0.3[a]	26.9	19.4±0.5[a]	0.44	2.7±0.02[a]	0.31	36.0±14.7[a]	2.4	10.7±0.5[a]	1.2
	760										
	1200	136.9±1.6[a]	26.1	19.5±0.4[a]	0.44	2.7±0.02[a]	0.31	97.0±18.3[b]	6.4	20.1±0.2[b]	2.2
P. acervalis	350										
	450	139.1±1.2	26.5	19.5±0.7	0.46	3.1±0.02	0.36	31.6±6.6	2.1	11.3±0.5	1.3
	760										
	1200										
A. carinata	350	23.6±1.5[a]	4.5	9.9±0.4[a]	0.22	1.8±0.02[a]	0.21	9.0±2.6[a]	0.6	3.2±0.5[a]	0.4
	450	28.5±2.4[b]	5.4	10.8±0.1[a]	0.24	1.9±0.01[a]	0.22	10.9±5.5[a]	0.7	6.0±0.5[b]	0.7
	760	33.1±1.2[b]	6.3	10.9±0.2[a]	0.24	1.8±0.01[a]	0.21	30.7±7.0[b]	2.0	8.5±0.6[c]	0.9
	1200	33.5±3.1[b]	6.4	10.6±0.5[a]	0.24	1.8±0.03[a]	0.21	46.4±2.1[b]	3.1	11.4±0.2[d]	1.3
A. gibbosa	350	27.8±0.5[a]	5.3	9.0±0.1[a]	0.20	1.7±0.01[a]	0.20	19.0±1.8[a]	1.3	2.7±0.5[a]	0.3
	450	25.9±0.6[b]	4.9	9.2±0.1[a]	0.21	1.7±0.02[a]	0.20	21.5±2.5[b]	1.4	3.4±0.5[a]	0.4
	760	28.2±0.7[a]	5.4	9.7±0.1[b]	0.22	1.7±0.02[a]	0.20	52.8±6.1[c]	3.5	7.1±0.6[b]	0.8
	1200	28.7±0.6[a]	5.5	9.6±0.1[b]	0.21	1.7±0.02[a]	0.20	85.8±11.3[d]	5.7	9.9±0.2[c]	1.1

Table 3. Overview of element to Ca ratios in foraminiferal calcite (Avg=average; SE=standard error) and partition coefficients D_E, with D_E of ambient conditions (treatment B) in bold. Letters ([a] to [d]) indicate (per species per E/Ca) groups that are statistical different (one-way ANOVA).

Species	Zn/Ca		Ba/Ca	
	R^2	p-value	R^2	p-value
S. marginalis	0.99	<0.0005	0.81	<0.025
A. angulatus	0.95	<0.0025	0.99	<0.0005
L. bradyi	0.98	<0.0005	0.97	<0.0025
A. carinata	0.98	<0.001	0.94	<0.005
A. gibbosa	0.99	<0.0005	0.98	<0.001

640 **Table 4. Regression and p-values of foraminiferal Zn/Ca and Ba/Ca versus pCO_2 values of**
641 **different species (Fig. 4).**